

Fabrication of Core–Shell Structure of M@C (M = Se, Au, Ag₂Se) and Transformation to Yolk–Shell Structure by Electron Beam Irradiation or Vacuum Annealing

Jixin Zhu,[†] Ting Sun,[†] Huey Hoon Hng,[†] Jan Ma,[†] Freddy Yin Chiang Boey,[†]
Xiongwen Lou,[‡] Hua Zhang,[†] Can Xue,[†] Hongyu Chen,[§] and Qingyu Yan^{*,†}

[†]School of Materials Science and Engineering and [‡]School of Chemical and Biomedical Engineering and [§]Division of Chemistry & Biological Chemistry, School of Physical and Mathematical Sciences, Nanyang Technological University, Singapore

Received May 21, 2009. Revised Manuscript Received July 2, 2009

Selenium @ carbon core–shell spheres have been synthesized via a simple one-step hydrothermal carbonization process using sucrose and sodium selenite as precursors. Metal selenide or noble metal, e.g. Ag₂Se or Au, can be easily encapsulated into the carbon shell by using the as-prepared Se@C core–shell samples as site templates. The transformation from core/shell to yolk/shell structure, e.g. Se@C, Au/Se@C and Ag₂Se@C, can be achieved through thermal evaporation under electron beam irradiation or vacuum annealing to evaporate Se. The optical absorption of the samples can be tuned by varying the structure/compositions of the samples.

1. Introduction

Colloidal micro/nanomaterials with controlled yolk–shell (YS) structures have attracted much attention in various advanced applications, e.g., drug delivery, photonic crystals, and catalyst.^{1–7} As compared to their single-component counterparts, such multicomponent system can possess multifunctional properties, which can be adjusted by manipulating their size, composition, morphology, phase, and interface functionality.^{5,8–13} Several approaches to achieve YS structures with controlled shell chemistry have been demonstrated, e.g., SiO₂¹² or

polymer.¹⁴ The synthesis of carbon-shell-based YS structures, however, has not been successful.^{4,15–17} Carbon coating is one of the most attractive shell layers because of its low preparation cost, chemical activity,¹⁸ and biocompatibility.¹⁹ Carbon coating also allows interface functionalization to serve as trapping sites for nanoparticle formation^{20,21} to induce specific catalytic, magnetic, electronic, optical properties.^{16,22,23} Moreover, the successful fabrication of YS structure with adjustable core size and chemistry can further extend their functionalities and applications.

In this study, we report a one-step green hydrothermal process for preparation of Se@C core–shell spheres. Encapsulation of metal selenide (Ag₂Se) and noble-metals, e.g., Au, with adjustable size in carbonaceous shells is demonstrated by allowing the Ag⁺ or Au³⁺ ions to diffuse through and react with the Se core. Furthermore, these multiple-layer core–shell structures can be transformed into YS structures with size-tunable cores by evaporating Se under electron beam irradiation (EBI) or vacuum annealing. It is shown that the optical absorption of the YS sphere is highly dependent on the detailed structures

*Corresponding author.

- (1) Lou, X. W.; Archer, L. A.; Yang, Z. C. *Adv. Mater.* **2008**, *20*, 3987.
- (2) Li, J.; Zeng, H. C. *Angew. Chem., Int. Ed.* **2005**, *44*(28), 4342–4345.
- (3) Kim, S. H.; Yin, Y. D.; Alivisatos, A. P.; Somorjai, G. A.; Yates, J. T. *J. Am. Chem. Soc.* **2007**, *129*(30), 9510–9513.
- (4) Harada, T.; Ikeda, S.; Ng, Y. H.; Sakata, T.; Mori, H.; Torimoto, T.; Matsumura, M. *Adv. Funct. Mater.* **2008**, *18*(15), 2190–2196.
- (5) Gao, J. H.; Liang, G. L.; Zhang, B.; Kuang, Y.; Zhang, X. X.; Xu, B. *J. Am. Chem. Soc.* **2007**, *129*(5), 1428–1433.
- (6) Huang, X. Q.; Guo, C. Y.; Zuo, L. Q.; Zheng, N. F.; Stucky, G. D. *Small* **2009**, *5*(3), 361–365.
- (7) Zhao, W. R.; Chen, H. R.; Li, Y. S.; Li, L.; Lang, M. D.; Shi, J. L. *Adv. Funct. Mater.* **2008**, *18*(18), 2780–2788.
- (8) Lou, X. W.; Yuan, C. L.; Rhoades, E.; Zhang, Q.; Archer, L. A. *Adv. Funct. Mater.* **2006**, *16*(13), 1679–1684.
- (9) Bergwerff, J. A.; Lysova, A. A.; Espinosa-Alonso, L.; Koptug, I. V.; Weckhuysen, B. M. *Chem.—Eur. J.* **2008**, *14*(8), 2363–2374.
- (10) Gao, J. H.; Liang, G. L.; Cheung, J. S.; Pan, Y.; Kuang, Y.; Zhao, F.; Zhang, B.; Zhang, X. X.; Wu, E. X.; Xu, B. *J. Am. Chem. Soc.* **2008**, *130*(35), 11828–11833.
- (11) Lee, J.; Park, J. C.; Song, H. *Adv. Mater.* **2008**, *20*(8), 1523.
- (12) Li, J. W.; Ding, Y. J.; Li, X. M.; Jiao, G. P.; Wang, T.; Chen, W. M.; Luo, H. Y. *Chem. Commun.* **2008**, *45*, 5954–5956.
- (13) Chen, M.; Kim, Y. N.; Li, C.; Cho, S. O. *J. Phys. Chem. C* **2008**, *112*(17), 6710–6716.
- (14) Xing, S. X.; Tan, L. H.; Chen, T.; Yang, Y. H.; Chen, H. Y. *Chem. Commun.* **2009**, *13*, 1653–1654.
- (15) Li, L.; Li, G. H.; Fang, X. S. *J. Mater. Sci. Technol.* **2007**, *23*(2), 166–181.

- (16) Wu, S. Y.; Ding, Y. S.; Zhang, X. M.; Tang, H. O.; Chen, L.; Li, B. X. *J. Solid State Chem.* **2008**, *181*(9), 2171–2177.
- (17) Yu, J. C.; Hu, X. L.; Li, Q.; Zheng, Z.; Xu, Y. M. *Chemistry—Eur. J.* **2006**, *12*(2), 548–552.
- (18) Stein, A.; Wang, Z. Y.; Fierke, M. A. *Adv. Mater.* **2009**, *21*(3), 265–293.
- (19) Guo, S. R.; Gong, J. Y.; Jiang, P.; Wu, M.; Lu, Y.; Yu, S. H. *Adv. Funct. Mater.* **2008**, *18*(6), 872–879.
- (20) Cui, R. J.; Liu, C.; Shen, J. M.; Gao, D.; Zhu, J. J.; Chen, H. Y. *Adv. Funct. Mater.* **2008**, *18*(15), 2197–2204.
- (21) Sun, X. M.; Liu, J. F.; Li, Y. D. *Chem—Eur. J.* **2006**, *12*(7), 2039–2047.
- (22) Sun, X. M.; Li, Y. D. *Langmuir* **2005**, *21*(13), 6019–6024.
- (23) Sun, S. H.; Jaouen, F.; Dodelet, J. P. *Adv. Mater.* **2008**, *20*(20), 3900.

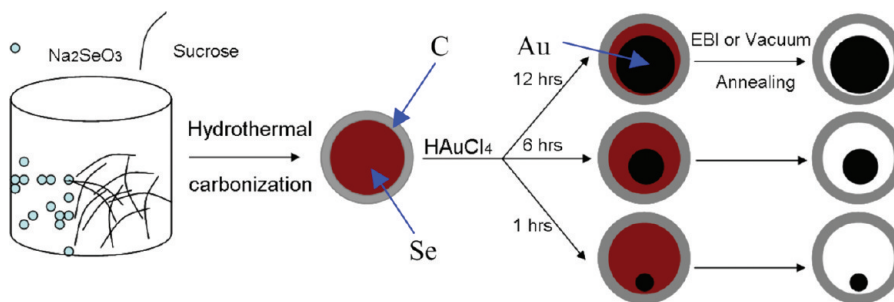


Figure 1. Schematic illustration of the major steps for preparing Au/Se@C yolk-shell structure.

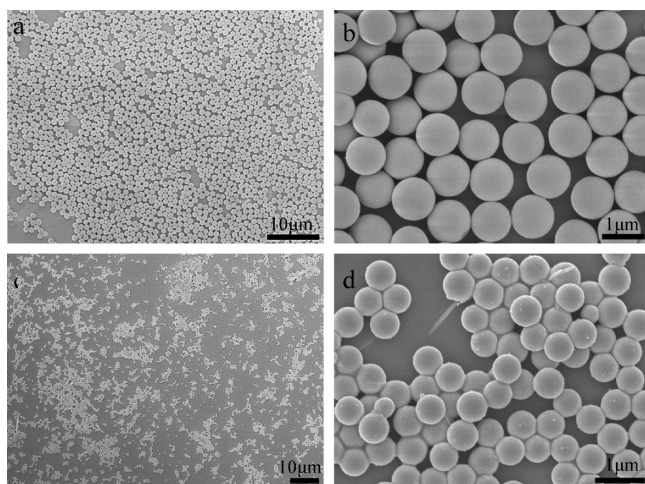


Figure 2. SEM of the Se@C samples prepared at different reaction temperatures, T , and reaction time, t , (a, b) $T = 180\text{ }^{\circ}\text{C}$, $t = 2.5\text{ h}$; (c, d) $T = 190\text{ }^{\circ}\text{C}$, $t = 2.5\text{ h}$.

and compositions. Such YS sphere may have various potential applications, e.g., sensors or catalysis.

2. Experimental Procedures

Preparation of Materials. *Se@C.* A typical process, 2 g sucrose was dissolved in 35 mL of Millipore water under stirring at room temperature, then 0.1 mmol Na_2SeO_3 was added into the solution to form a clear solution. The mixture was transferred into a 40 mL of autoclave and maintained at $180\text{ }^{\circ}\text{C}$ for 2.5 h. The temperature is controlled through the external oven that the autoclave was put in. The Se@C core-shell structured particles were collected by centrifugation, and washed with ethanol and water several times and dispersed in Millipore Water.

Au/Se@C. One-half a milliliter of 40 M aqueous HAuCl_4 solution was added into 1 mL of fresh as-prepared Se@C solution under stirring at $60\text{ }^{\circ}\text{C}$ for different reaction time. The particles were then washed with ethanol several times.

Ag₂Se/Se@C. Eight milligrams of AgNO_3 and 5 mg of sucrose were added into 1 mL of as-prepared Se@C in Millipore water solution under stirring at room temperature for 4 h, and then washed with ethanol several times.

Yolk-Shell Structure Formation. The samples prepared with core-shell structure were irradiated with electron beam in the TEM with controlled beam size

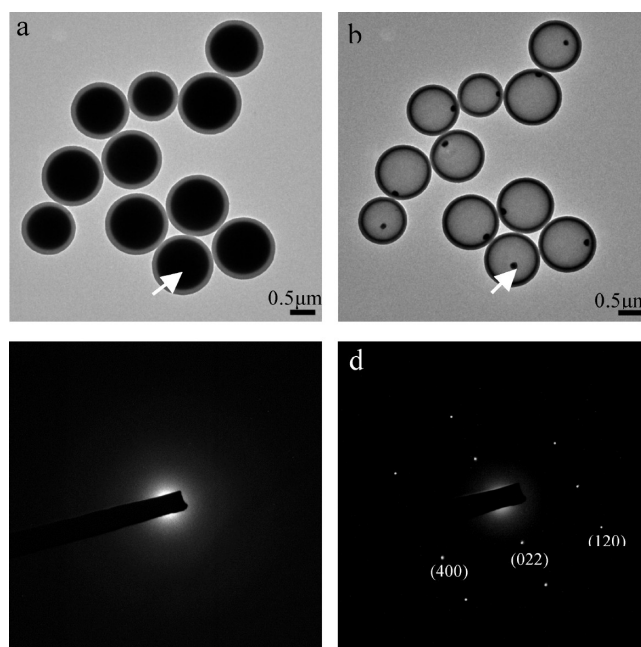


Figure 3. (a, b) TEM images of Se@C with core-shell and yolk-shell structures; (c, d) SAED patterns obtained on the Se core arrowed in (a) and (b), respectively.

and irradiation time to form the yolk-shell structure in situ. Or the YS structure can be formed by annealing the core-shell samples in a vacuum furnace at $T = 500\text{ }^{\circ}\text{C}$ and $P = 2\text{--}3 \times 10^{-6}\text{ Torr}$ for 30 min.

Characterization. The morphology of the as-synthesized M@C spheres was investigated by using a field-emission SEM (FE-SEM; JEOL, JSM-6340F). For TEM observation, the suspension was dropped onto the copper grid and dried at room temperature. A TEM (JEOL, JEM-2010) operating at 120 kV was used to characterize the nanostructures. Energy dispersive X-ray (EDX) analysis was carried out in the TEM (JEOL, JEM-2010). A Scintag PAD-V X-ray diffractometer with a Cu $\text{K}\alpha$ source was used for phase identification. UV-vis absorption spectroscopy was performed with a Hitachi U-3010 spectrophotometer.

3. Results and Discussion

A schematic illustration of the representative steps for preparing the Au/Se@C yolk-shell structure is shown in Figure 1. A typical synthesis is achieved by dissolving sucrose and sodium selenite into Millipore water and

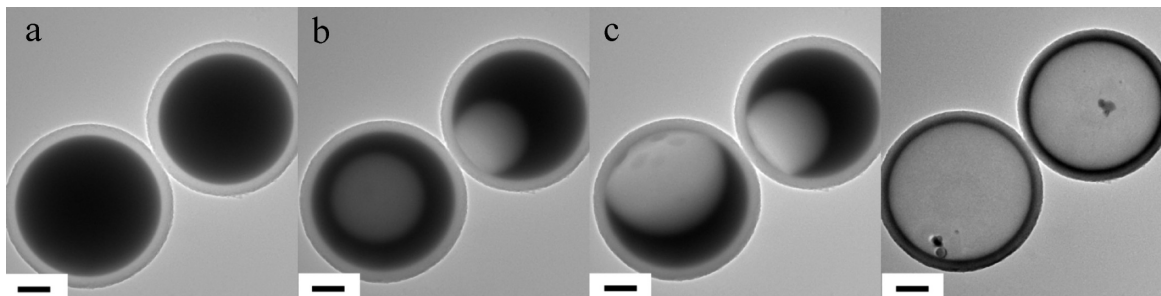


Figure 4. (a–d) Transformation process of Se@C from core–shell to yolk–shell structure under electron beam irradiation. (All scale bars are 0.2 μm).

heating it in an autoclave at 180 $^{\circ}\text{C}$ for 2.5 h to prepare uniform Se@C core–shell particles. The transformation of Se@C core–shell structures to Au/Se@C and Ag₂-Se@C YS structures with controlled core size and composition was achieved by allowing the Au³⁺ or Ag⁺ ions to diffuse through the carbon shell to react with the Se core, and finally evaporating the remaining Se under electron beam irradiation (EBI) in TEM or vacuum annealing.

Figure 2 shows the as-prepared Se@C spheres synthesized at different temperatures. It reveals that the particles prepared at 180 $^{\circ}\text{C}$ (see images a and b in Figure 2) have an average diameter of $\sim 1 \mu\text{m}$ with a narrow size distribution. These particles are spherical with smooth surfaces. Increasing the synthesis temperature to 190 $^{\circ}\text{C}$ leads to the formation of particles with smaller size, e.g., 600 nm (see images c and d in Figure 2), which is possibly due to the faster nucleation process.²⁴ Energy-dispersive X-ray (EDX) analysis (see the Supporting Information, Figure S1) confirms the existence of both Se and C. The X-ray diffraction (XRD) result (see the Supporting Information, Figure S2), however, shows no noticeable Bragg peaks, indicating no long-range ordered crystal structure, whereas a broad peak at 15–40 $^{\circ}$ corresponding to the amorphous carbon structures is observed.^{16,25}

Bright-field transmission electron microscopy (TEM) images (see Figure 3) show complementary contrast, confirming the formation of core–shell structures. In the case of particles with an average diameter of $\sim 1 \mu\text{m}$, it can be observed that the spherical core is in the range of 800–900 nm covered by a uniform layer of secondary phase of a thickness of ~ 100 nm. The selected area electron diffraction (SAED) pattern (Figure 3c) performed on the core (arrow indicated in Figure 3a) exhibits diffused rings corresponding to the amorphous structures consistent with the XRD results. The as-prepared core–shell structures are observed to transform to yolk–shell structure with core size ~ 100 nm (see Figure 3b) under EBI as a result of thermal evaporation.^{26,27} The SAED on the remaining core (arrow indicated in Figure 3b) corre-

sponds to single-crystalline Se with a hexagonal lattice structure. Thus, based on the above observation, we conclude that the initial particles are Se@C core–shell structures. The as-prepared Se cores are amorphous. They have a relatively high vapor pressure and hence can be easily evaporated through the carbon shell under EBI. The carbon shells, however, show no obvious morphological change under EBI. Besides the EBI process, we also used vacuum annealing to prepare similar YS structures (see the Supporting Information, Figure S3) for the purpose of bulk production. The products show a thicker shell than those obtained through EBI. This is possibly because more residual Se condenses onto the carbon shell after the annealing process.

On the basis of all the above observations, we further investigated the kinetics of the transformation of Se core. The time-dependent morphological changes of the Se@C particles under EBI are illustrated in Figure 4. The thermal energy from EBI has two major effects on the Se cores: first to cause the vaporization of the Se through the amorphous carbon shell and second to crystallize the remaining Se in the carbon shell. Once the Se becomes crystalline, it remains stable under the EBI. The remaining crystalline Se exists as a thin layer attached to the inner wall of the carbon shell and as a small core inside carbon shell, as confirmed by the EDX line-scan (see Figure S4 in the Supporting Information), which leads to the formation of the YS structure.

The Se cores can serve as sacrificial templates for importing noble metals, Au or Ag, into the carbonaceous shell.¹ For example, by mixing the Se@C samples with HAuCl₄ in aqueous solution, Au³⁺ ions can permeate through the amorphous carbon shell and be reduced by the amorphous Se.²⁸ Although the morphology of the samples shows no obvious difference (see Figure 5a and b), the chemistry of the cores has changed to Au/Se mixture as indicated by EDX measurements. Under EBI, the core–shell structures change to yolk–shell structure because of the evaporation of Se, whereas the EDX measurement suggests there is still remaining Se in the YS spheres (see image c and panel k in Figure 5). The SAED of the Au core shows ring patterns indicating the polycrystalline nature of the Au cores (see Figure 5l). The amount of Au in the cores as well as the size of the cores in the YS structures can be adjusted by varying the reaction

(24) Chen, M.; Liu, J. P.; Sun, S. H. *J. Am. Chem. Soc.* **2004**, *126*(27), 8394.

(25) Su, F. B.; Lee, F. Y.; Lv, L.; Liu, J. J.; Tian, X. N.; Zhao, X. S. *Adv. Funct. Mater.* **2007**, *17*(12), 1926–1931.

(26) Tian, L.; Yang, X. F.; Lu, P.; Williams, I. D.; Wang, C. H.; Ou, S. Y.; Liang, C. L.; Wu, M. M. *Inorg. Chem.* **2008**, *47*(13), 5522–5524.

(27) Yin, Y. D.; Rioux, R. M.; Erdonmez, C. K.; Hughes, S.; Somorjai, G. A.; Alivisatos, A. P. *Science* **2004**, *304*(5671), 711–714.

(28) Mayers, B.; Jiang, X. C.; Sunderland, D.; Cattle, B.; Xia, Y. N. *J. Am. Chem. Soc.* **2003**, *125*(44), 13364–13365.

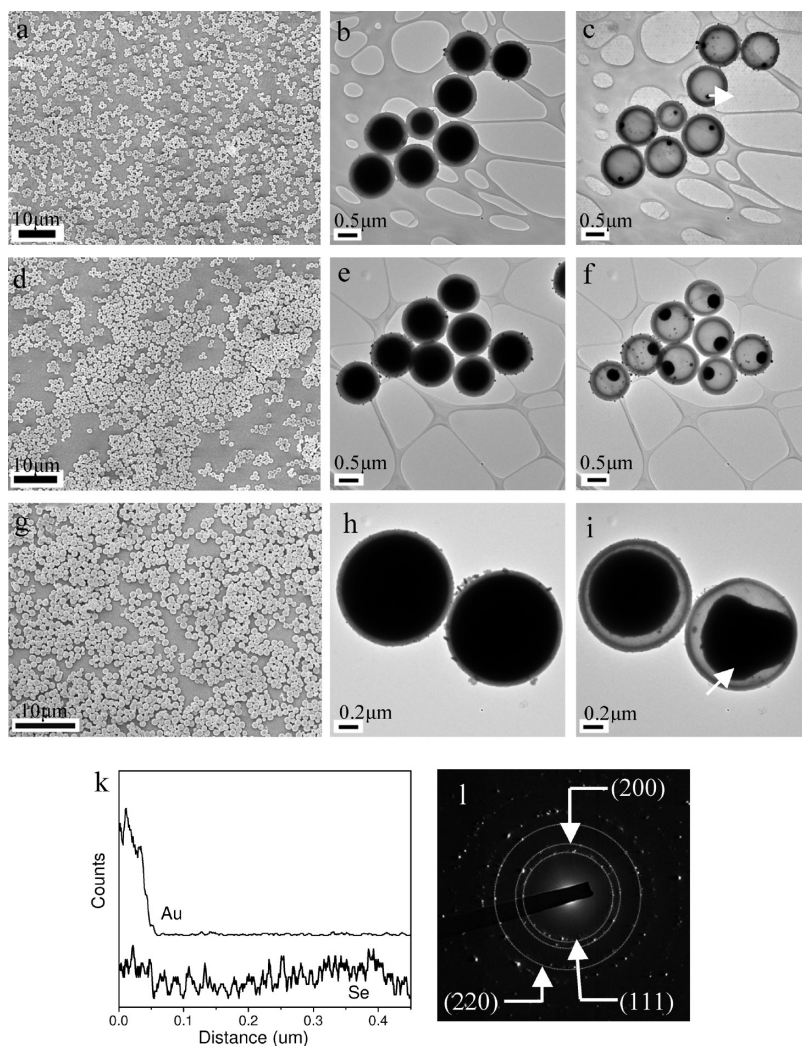


Figure 5. SEM and TEM images of Au/Se@C obtained with different reaction time: (a, b) 1, (d, e) 6, and (g, h) 12 h; (c, f, and i) corresponding TEM images of Au/Se@C yolk-shell structure; (k) EDX line scan along the line arrowed in c; and (l) SAED corresponding to the core arrowed in i.

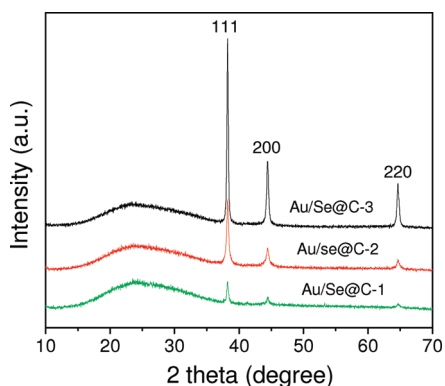


Figure 6. X-ray diffraction patterns of Au/Se@C samples.

time of the Se@C samples in HAuCl_4 solution, e.g., by extending the reaction time, t_{HAuCl_4} , the Au cores increased from 120 to 900 nm (see Figure 5d–i) under EBI. It is also noticed that the Au nanoparticles can form on the surface of the Se@C samples, possibly because of the reduction of HAuCl_4 at elevated temperature (see Figure 5e). In the case for the preparation of bulk amount of Au/Se@C YS particles, vacuum annealing can be applied instead.

Figure 6 shows the X-ray diffraction patterns of the as-prepared Au/Se@C core-shell samples with different t_{HAuCl_4} . Here, the samples are noted as Au/Se@C-1 for $t_{\text{HAuCl}_4} = 1$ h, Au/Se@C-2 for $t_{\text{HAuCl}_4} = 6$ h and Au/Se@C-3 for $t_{\text{HAuCl}_4} = 12$ h. The Bragg peaks in the 2θ range of $35\text{--}70^\circ$ confirm the existence of the face-centered cubic Au (JCPDS No. 65–2870) phase, while the broad peak in the 2θ range of $15\text{--}35^\circ$ is attributed to the amorphous carbon shell.^{16,23} Using Scherrer's equation, we determined the crystallite sizes of all three types of samples obtained with different t_{HAuCl_4} from the peak width of their respective XRD patterns. The crystallite sizes of all the samples are similar, ~ 26 nm. This calculated crystal size is much smaller than the actual core size observed in TEM images (see Figure 5c, f, and i), which is consistent with the polycrystalline nature of the Au as indicated by the SAED results (see Figure 5l).

Beside Au/Se@C YS structures, similar process can also be used to obtain $\text{Ag}_2\text{Se@C}$ YS structures (see Figure 7a–d and the Supporting Information, Figures S5 and S6) by allowing Se@C samples to react with AgNO_3 . The Ag^+ ions react with amorphous Se under

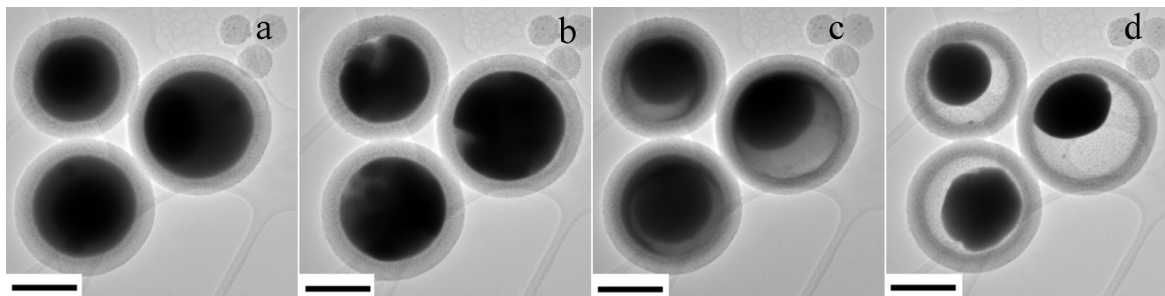


Figure 7. The transformation process of $\text{Ag}_2\text{Se}/\text{Se}@C$ from core-shell to yolk-shell structure under electron beam irradiation (all scale bars are $0.5 \mu\text{m}$).

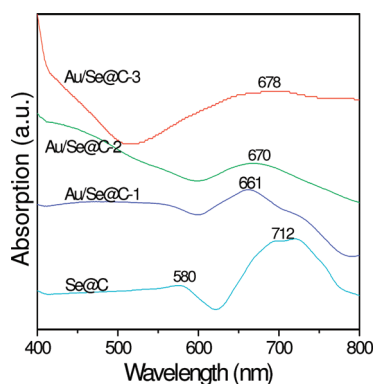


Figure 8. UV-vis absorption spectra of the $\text{Se}@C$, $\text{Au}/\text{Se}@C-1$, $\text{Au}/\text{Se}@C-2$, and $\text{Au}/\text{Se}@C-3$ samples.

reducing environments²⁹ because of the presence of sucrose.^{30,31} Such a process opens up the possibility of forming YS structures composed of Se-based semiconductors cores, e.g., CdSe , PbSe , ZnSe , etc., to introduce multifunctionalities for different applications. The XRD pattern (see the Supporting Information, Figure S7) of the as-prepared $\text{Ag}_2\text{Se}/\text{Se}@C$ core-shell particles shows only Bragg peaks from Ag_2Se with orthorhombic structure; the broad amorphous backgrounds in the low-angle region are from the carbon shell.

The UV-vis absorption spectra (see Figure 8) of the $\text{Au}/\text{Se}@C$ core-shell colloids with different t_{HAuCl_4} values show the presence of signature peaks from both Au and Se. The spectra obtained from $\text{Se}@C$ samples show strong absorption peaks at 712 and 385 nm, which are attributed to the presence of Se.^{32,33} The absorption

spectrum of the dispersion of amorphous Se colloids is not only highly dependent on the size but also varies for different distribution in the particles.³⁴ The absorption peak at ~ 660 nm is attributed to the Au core, which shows a red shift from 661 to 678 nm with the increase in particle size.^{35,36}

4. Conclusion

In this study, nearly monodisperse $\text{Se}@C$ core-shell spheres were prepared by a facile hydrothermal route. The as-prepared $\text{Se}@C$ particles can be further transformed to yolk-shell structure through electron beam irradiation or vacuum annealing, through which the Se cores are partially evaporated and the remaining part becomes crystalline with higher thermal stability. The Se core can react with either HAuCl_4 or AgNO_3 to form Au or Ag_2Se inside the carbon shell, whereas the samples can be further transformed into $\text{Au}/\text{Se}@C$ or $\text{Ag}_2\text{Se}/\text{Se}@C$ yolk-shell structures by EBI or vacuum annealing. The size of the cores in these cases, e.g., $\text{Au}/\text{Se}@C$ or $\text{Ag}_2\text{Se}/\text{Se}@C$ YS structures, can be controlled by adjusting the reaction parameters. It is possible to extend this synthesis protocol to form multifunctional YS particles, e.g., $\text{PbSe}@C$, $\text{ZnSe}@C$, $\text{CdSe}@C$, etc., for catalytic, magnetic, and optical applications.

Acknowledgment. The authors gratefully acknowledge the AcRF Tier 1 RG 31/08 from MOE, Singapore.

Supporting Information Available: EDX spectra and line scan of $\text{Se}@C$, $\text{Au}/\text{Se}@C$, and $\text{Ag}_2\text{Se}/\text{Se}@C$ core-shell and yolk-shell structures; SEM and TEM images of $\text{Se}@C$, $\text{Au}/\text{Se}@C$, and $\text{Ag}_2\text{Se}/\text{Se}@C$ YS structures; XRD of $\text{Se}@C$, $\text{Ag}_2\text{Se}/\text{Se}@C$ core-shell structures (PDF). This material is available free of charge via the Internet at <http://pubs.acs.org>.

(29) Camargo, P. H. C.; Lee, Y. H.; Jeong, U.; Zou, Z. Q.; Xia, Y. N. *Langmuir* **2007**, *23*(6), 2985–2992.

(30) Yan, Q. Y.; Chen, H.; Zhou, W. W.; Hng, H. H.; Boey, F. Y. C.; Ma, J. *Chem. Mater.* **2008**, *20*(20), 6298–6300.

(31) Yan, Q. Y.; Raghuvver, M. S.; Li, H. F.; Singh, B.; Kim, T.; Shima, M.; Bose, A.; Ramanath, G. *Adv. Mater.* **2007**, *19*(24), 4358.

(32) Mayers, B. T.; Liu, K.; Sunderland, D.; Xia, Y. N. *Chem. Mater.* **2003**, *15*(20), 3852–3858.

(33) Lin, Z. H.; Wang, C. R. C. *Mater. Chem. Phys.* **2005**, *92*(2–3), 591–594.

(34) Watillon, A.; Dauchot, J. J. *Colloid Interface Sci.* **1968**, *27*(3), 507.

(35) Amendola, V.; Meneghetti, M. *J. Phys. Chem. C* **2009**, *113*(11), 4277–4285.

(36) Halder, A.; Ravishankar, N. *Adv. Mater.* **2007**, *19*(14), 1854.